

To represent the potential impacts of dams and irrigation on river flow, we constructed a two-part Mekong Water Management” (MWMM) sub-model, representing the interaction between water flows and the physical infrastructure of the water resources system reflected in reservoir operating policies and irrigation demand.

The MWMM operates on a monthly time scale and is driven by streamflow data simulated by the VIC model. VIC-simulated streamflow represents the input to the dam, and the MWMM computer program computes updated dam storage and outflow rates for each month. In the case of dams used for irrigation, the MWMM accounts for irrigation extractions, if the current storage in the dam is sufficient to meet the irrigation demand in that month.

Hydro-electric power dams in the Mekong include many run-of-the-river dams, which do not appreciably affect the river flow, and were not included in the MWMM. The dams contemplated by the MWMM are assumed to operate differently in the wet and dry seasons. The storage reservoir is allowed to be filled during the wet season, while in the dry season water is released from storage as needed to fulfill irrigation demands. Since information about the operating policies was not available, simple rule curves were assumed.

In the case of hydropower dams, a minimum storage level was imposed, to produce the minimum flow rate necessary for operation of the dam. The operational target to be met by these dams in the MWMM was the observed (or designed) power output. If the dam is also used for irrigation as well as hydropower, operational targets in the MWMM were the observed (or designed) irrigation releases combined with the power output. We used simulated irrigation demands, as described further below.

In order to convert between storage volume and storage level in a reservoir, the MWMM assumes its cross-section to be rectangular. In result, storage level varies linearly with volume, between the specified minimum (required for dam operation) and maximum levels. The power generated at each dam is a function of the rate at which flow passes through the turbines, and the head associated with this flow, determined by the storage level.

$$\text{power} = \rho \eta g h Q$$

where, ρ = density of water,

g = acceleration due to gravity,

h = hydrostatic pressure head associated with of the inflow Q ,

η = efficiency of the power generating system.

Irrigation. Simulation of irrigation in the Mekong basin was carried out under the simplest assumptions, in the absence of data on actual irrigation water use. The irrigation model has not been validated, which will be the subject of future work.

The irrigation model uses a modified VIC code in which the moisture of top soil layer in an irrigated crop area is not allowed to drop below a user-specified fraction of the soil’s saturation level. In the normal operation of VIC, the moisture level of each soil layer fluctuates in response to the time-variable precipitation and evapo-transpiration

rates. In the modified VIC code (irrigation model), this moisture level is still allowed to fluctuate, but is never allowed to drop under a fixed, user-specified elevated level. This simulates the effect of the addition of irrigation water during periods where rainfall alone would not be able to maintain the desired high moisture level in the soil. An arbitrary value of 90% saturation was used in our model runs, deemed to be close to saturation but not impose a requirement for perfect irrigation to permanently maintain saturation conditions.

Only some of the model grid cells contain irrigated crops. The cells which do contain irrigated crops were determined by the AVHRR-OGE class 37, “hot irrigated cropland”. A cell which has this class 37 is assumed to possibly be only partly covered by irrigated rice. The fraction of a cell of class 37 which is covered by irrigated rice was determined based on the estimates for the total area of irrigated rice cultivation of the International Rice Research Institute (IRRI) for the specific country, shown in table 2.1.1 below. (In this way, for a country completely included inside the basin, the total surface area of irrigated rice would agree with the IRRI data.)

Because we have IRRI estimates of area covered by irrigated rice crops only for 1995 and 2000, we obtained estimates of this area for each country based on the total rice crops FAOSTAT data (shown in Table 2.4, where dashes indicate missing data), assuming that the percentage of total rice which is irrigated rice remained constant in 1979-1995, at 2000/2001 levels (20% of total rice for Thailand, and 14.5% for Laos). For Cambodia, IRRI data for 1995 indicated 8% of rice being irrigated rice, and this value was used for 1979-1995 (rather than the 15% computed from Table 2.4. and Table 2.5). In the case of Vietnam, almost all of the irrigated rice is located on or near the Mekong delta.

Table 2.4. Area (ha) covered by irrigated rice, per country and per year (1979-2001), according to the Irrigated Rice Institute (in <http://www.irri.org/science/ricestat/index.asp>).

Year	Thailand	Cambodia	Lao PDR	Vietnam	Burma
2001	1,960,000	291,360	104,580	3,975,000	1,950,000
2000	-	-	-	-	-
1999	-	-	-	-	1,818,000
1998	-	-	-	-	1,593,000
1997	-	-	-	3,725,000	1,557,000
1996	1,894,000	-	-	3,572,000	1,535,000
1995	1,257,000	-	-	3,527,000	1,767,000
1994	-	-	-	3,495,000	1,592,000
1993	-	-	-	3,440,000	1,338,000
1992	2,206,000	-	-	3,405,000	957,000
1991	-	-	-	3,336,000	835,000
1990	2,067,000	-	-	3,195,000	869,000
1989	2,485,000	-	-	3,141,000	852,000
1988	2,338,000	-	-	2,639,000	835,000
1987	2,390,000	-	-	2,564,000	798,000
1986	2,376,000	-	-	2,539,000	875,000
1985	2,376,000	-	-	2,510,000	858,000
1984	2,307,000	-	-	2,490,000	861,000
1983	2,111,000	-	-	2,430,000	838,000
1982	2,180,000	-	-	2,380,000	805,000
1981	2,100,000	-	-	2,310,000	865,000
1980	2,006,000	-	-	2,250,000	873,000
1979	2,022,000	-	-	2,190,000	833,000

Table 2.5. Area (ha) covered by rice paddies, per country and per year (1979-2000), according to FAOSTAT.

Year	Thailand	Cambodia	Lao PDR	Vietnam	Burma
2000	9,761,120	1,903,159	719,370	7,666,300	6,302,492
1999	9,969,920	2,079,442	717,577	7,653,600	6,210,787
1998	9,511,520	1,962,566	617,538	7,362,700	5,458,500
1997	9,912,790	1,928,689	599,400	7,099,700	5,408,300
1996	9,267,200	1,864,000	553,741	7,003,800	5,768,500
1995	9,112,951	1,924,000	559,900	6,765,600	6,032,700
1994	8,975,229	1,494,600	610,960	6,598,600	5,742,875
1993	8,482,400	1,823,625	538,686	6,559,400	5,486,812
1992	9,159,680	1,685,400	565,749	6,475,400	5,056,200
1991	9,052,960	1,719,000	556,878	6,302,700	4,575,000
1990	8,791,885	1,855,000	663,600	6,042,800	4,760,000
1989	9,879,040	1,861,000	596,160	5,911,200	4,732,400
1988	9,905,932	1,825,000	524,828	5,740,800	4,527,300
1987	9,147,076	1,370,000	542,018	5,603,100	4,482,800
1986	9,194,021	1,520,000	641,632	5,703,100	4,665,700
1985	9,833,074	1,450,000	663,487	5,718,300	4,660,800
1984	9,629,710	978,000	655,095	5,675,000	4,601,300
1983	9,606,013	1,612,000	694,347	5,611,700	4,659,200
1982	8,940,017	1,615,000	736,812	5,711,700	4,562,300
1981	9,105,026	1,317,000	745,062	5,651,900	4,808,700
1980	9,200,080	1,400,000	732,050	5,600,200	4,800,900
1979	8,654,000	744,000	689,300	5,485,200	4,441,900

Each grid cell of class 37 is then split into two grid cells, which are modeled separately: a larger cell covered by non-irrigated rice, and a smaller cell covered by irrigated rice (the “irrigated cells”). The irrigation model is run only for the latter type of cell. This scheme is similar to that used by Haddeland et al (2003), although those authors represent sprinkle irrigation (in their simulations, irrigation water is added to the rainfall variable in the VIC runs).

The irrigation model (modified VIC code) was run for the entire simulation period (1979-2000) for the irrigated cells, imposing a 90% level of soil moisture saturation in the irrigated areas. The purpose of this model run is to estimate the evapo-transpiration losses, and sub-surface flow losses (which are smaller in magnitude) that result from maintaining such a high saturation level. The daily record of these water losses represents the “daily water demand” of the irrigation grid cell. Daily water demands are then compared against daily rainfall. If the daily rainfall volume is at least as large, then the water demand is met without an irrigation demand. In days when rainfall volume is less than the daily water demand, the difference is registered and represents the “daily irrigation demand”.

The model then attempts to meet the irrigation water demand of the grid cell by abstracting water from a nearby stream. Given the size of our grid cells (approaching 100 km²), every grid cell is assumed to contain streams in it. Therefore, at each daily time step, the irrigation model (modified VIC code) attempts to meet the irrigation water demand in the cell by subtracting it from the cell’s runoff volume. It is the depleted

runoff (after irrigation abstraction) which is then routed through the flow network by the routing model described in section a) above.

In periods of low rainfall, it is often the case that daily rainfall and runoff volumes in the grid cell are not sufficient to meet irrigation water demands. The unmet irrigation water demand in the downstream vicinity of a dam that is used for irrigation purposes is then used in the MWM model described above. The “vicinity” of the dam was arbitrarily set to a distance of 20 km (two model grid cells).

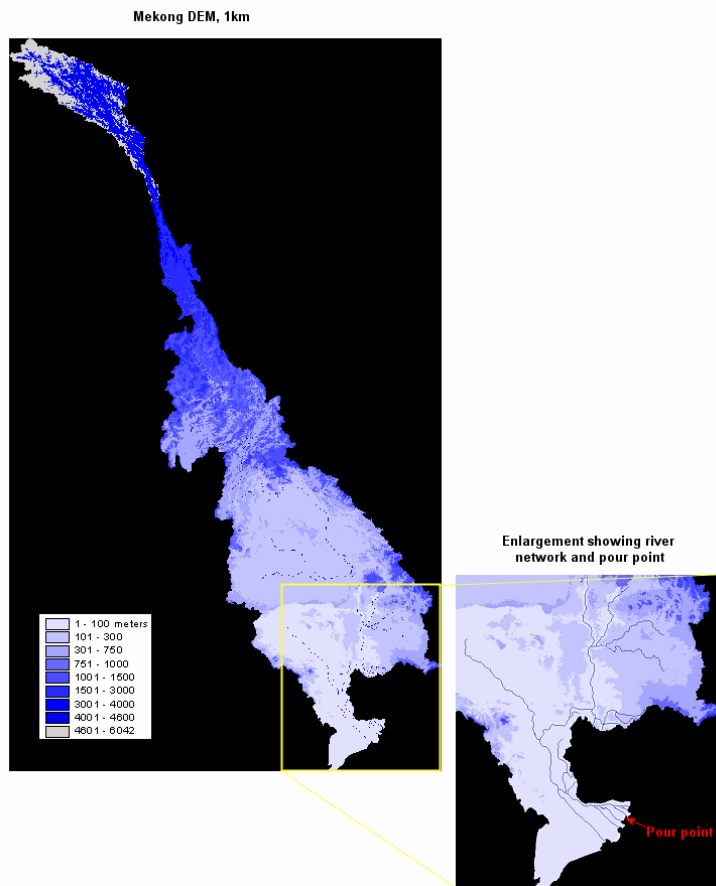


Figure 2.54. Elevations in the Mekong basin, from the GTOPO30 DEM (30 arc-second resolution), and main channels of the network computed from this DEM using Arc-Info

2.2.7.2 Development of the Geospatial Model of the Mekong Basin

a) Flow Network. The flow network is defined by the collection of flow direction from each model grid cell to one of its neighbors are known, then runoff from each grid cell can be routed through a sequence of grid cells forming a connected flow path that leads to the basin outlet. Flow routing through the flow network allows computing a hydrograph (the rate of flow varying over time) for any chosen point along a stream, such as a point where a stream gauge is located. It also allows the delineation of the sub-basin that contributes flow to any given point in a channel, composed of the point’s “upstream cells”.

Flow directions are determined by terrain topography, and a variety of computerized methods are available for deriving a stream network from a digital elevation model (DEM, Fig. 2.54). Our model grid cells are defined by parallel and meridian lines with a spacing of 5 arc minutes (1/12 of a degree) of latitude and longitude – roughly, 10 x 10 km at low latitudes. The method which we found to produce a network at this resolution with closest resemblance to the observed stream network involved using a DEM with the finer resolution of 30 arc seconds, or about 1 x 1 km). We used the DEM from the GTOPO30 dataset (<http://edcdaac.usgs.gov/topo30/topo30.html>).

Flow directions and the basin area that is drained through each grid cell (the “upstream area”, often also designated “accumulated flow”) were computed for each grid cell of the GTOPO30 DEM using the computational routines of the commercial program *Arc-Info*, which are based on the method by Jenson and Domingue (1988). Due to the large number of 1-km grid cells, a map of this complete stream network would contain too many lines for useful visualization. Fig. 2.55A shows the major stream lines of the computed network overlaid on a map of terrain elevations. In Fig. 2.55A, all lines having more than 10 upstream grid cells are shown. Fig. 2.55B shows the observed stream lines, from the Digital Chart of the World River Network Dataset (www.maproom.psu.edu/dcw/). The estimated lines in compare well with the observed lines. Note that the Tonle Sap lake is artificially represented as a channel in the computed network, and is absent from the map of observed stream lines.

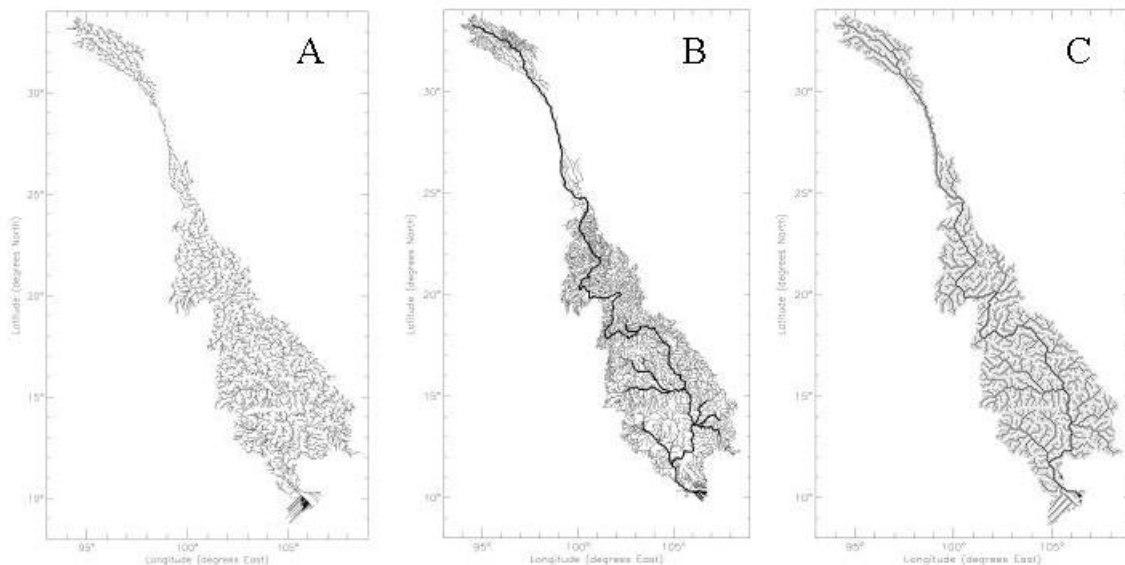


Figure 2.55. (A) Mekong stream network at 30 arc-second resolution (about 1 km) derived from the GTOPO30 DEM using Arc-Info; (B). Observed streams of the Mekong from Digital Chart of the World dataset; (C) Mekong 10 km resolution stream network obtained from the 1 km network in Fig. 2.51, using the 'upsampling' technique

Aggregating the DEM to the desired 5 arc minutes resolution (about 10 x 10 km) and again running the same *Arc-Info* routines to derive a network at that resolution, produced sub-optimal results, as is often the case with coarser-resolution DEM. The best results were obtained with a novel technique by which our 1-km network was “upscaled” to 10-km resolution. The technique is composed of the following steps. First, for each 10-km cell, the maximum value of accumulated flow in the one-hundred 1-km cells that fall within it was registered (variable f_{max}). Second, the flow direction of each 10-km cell was defined to be in the direction of the neighbor cell with the highest value of f_{max} . Third, these flow directions were used to compute new values of accumulated flow for the 10-km cells. Fourth, new flow directions for each 10-km cell was computed anew from the new values of accumulated flow. The third and fourth steps were then repeated another two times. Further iteration of these steps produced no more changes in the network. The rationale of this technique will be explained elsewhere (*Costa-Cabral, in preparation*).

The resulting network at 10-km resolution is shown in Fig. 2.55C. For easier comparison with the observed network, the two are overlaid in Fig. 2.56, showing the lower part of the basin. The agreement is overall good, with a few local discrepancies. Discrepancies were judged too small for perceptively influencing the simulated hydrographs, and no manual corrections of the network were performed. Like the 1-km network from which it was derived, the Tonle Sap lake is represented as a channel.

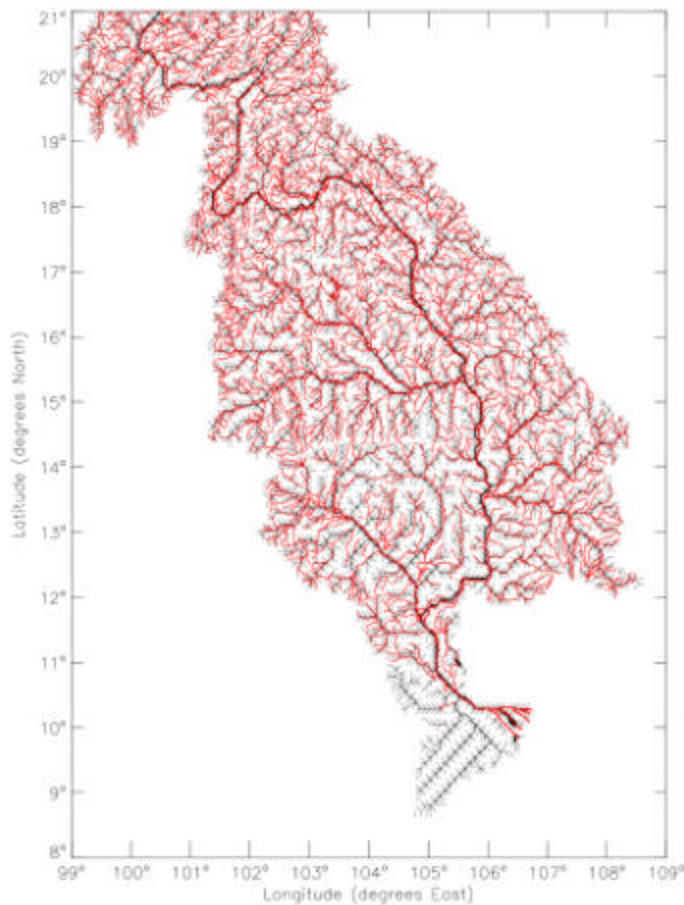


Figure 2.56. Stream network at 10-km resolution (in black) and observed stream network (in red) illustrated for the lower Mekong

b) Elevation Bands. In the VIC model, sub-grid variability in temperature, precipitation and snow accumulation is represented using elevation bands. The number of elevation bands in a grid cell depends on the range of elevations within that grid cell, calculated from the elevations of the finer resolution 30 arc-second DEM (represented in Fig. 2.51) Each elevation band was defined so as to cover a range of elevations of at most 300 meters.

c) Soils. The requirement for “soils” in VIC is to describe the physical properties of the soil relative to water movement (Fig. 2.57). The soil data and its processing followed methods reported by Nijssen et al. (2001a), and this section largely follows Section 3.b.2 of that reference. Soil textural information and bulk densities were obtained by application of the SOILPROGRAM of Carter and Scholes (1999) which combines the 5-minute FAO/UNESCO digital soil map of the world (FAO, 1995) with the World Inventory of Soil Emission Potentials (WISE) pedon database (Batjes, 1995). The FAO digital soil map records the dominant soil type for each 5-minute (roughly 10 km) grid cell, while the WISE database contains attributes for a large number of soil profiles around the globe. The SOILPROGRAM assigns attributes for each soil type by sampling the WISE database. The program allows specification of the depth of each soil horizon for which attributes are to be determined. The combined depth of the three soil layers was initially chosen as 1.5 m. The upper layer was taken as 0.1 m and the second layer as 1.0 m.

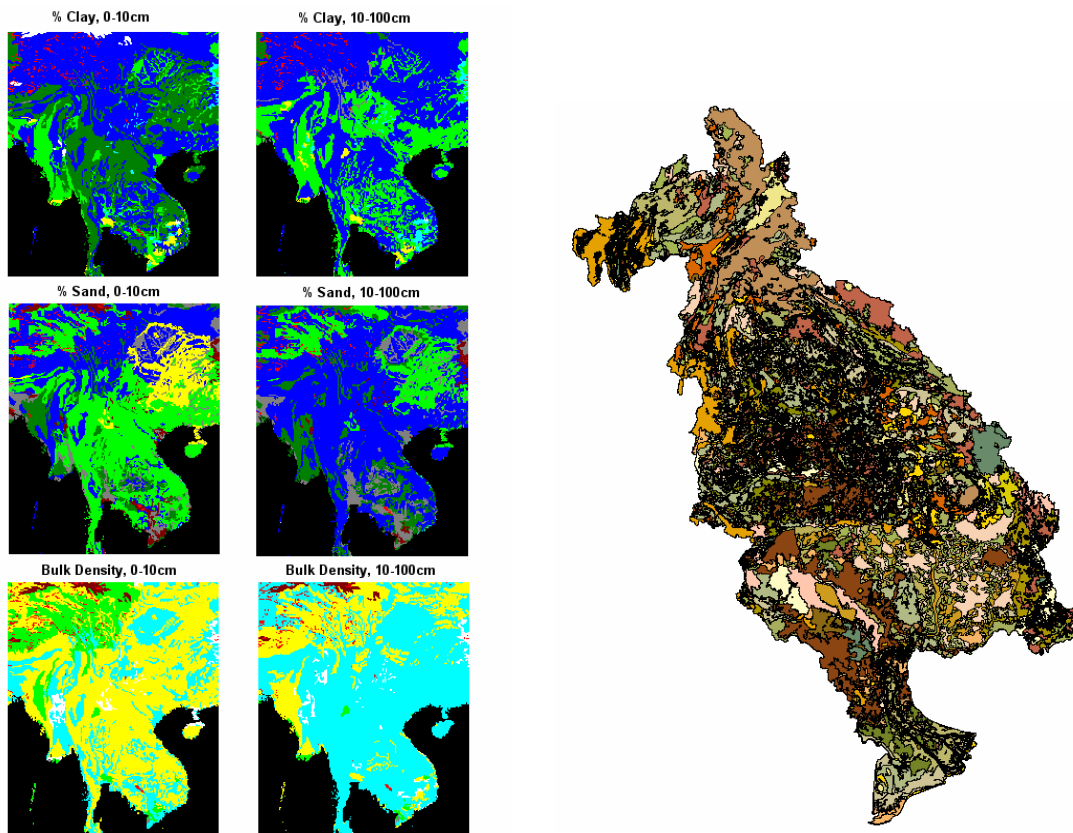


Figure 2.57. (left panel) Mekong soils at 5 resolution, from IGBP SoilData program (right panel) higher resolution soils data from the Mekong River Commission, for the "next" level of model development

The depth of the third layer was equivalent to 100 mm of water storage, which corresponds to a depth of about 0.25 m, depending upon the porosity. The depth of the second soil layer is a calibration parameter and it was changed during the process of calibration. Once the processing was completed at 5-minute resolution, soil attributes were aggregated to ¼ degree by taking an arithmetic average over all 5-minute pixels in the VIC grid cell. The remaining soil characteristics, such as porosity and saturated hydraulic conductivity, were based on Cosby et al. (1984).

The moisture contents at field capacity and wilting point were determined by calculating the moisture retention at a metric pressure of -33 kPa and -1500 kPa, respectively. The program TRIANGLE, from Gerakis (1999), was used to convert soil textural information to the United States Department of Agriculture (USDA) soil textural classes used by Cosby et al. (1984). The ARNO parameters at ¼ degree spatial resolution were obtained by interpolating the 20 x 20 parameters from Nijssen et al. (2001a) to the ¼ degree model grid cells. We are now developing a comparable dataset, at high resolution, with data directly from the Mekong River Commission (MRC).

d). *Vegetation and Land Use.* The requirements for vegetation and land use are not for knowing the “type” of vegetation per se, but rather what a set of hydrologic attributes are that correspond to (identifiable) vegetation classes. Land use throughout the Mekong basin has undergone important changes in the last several decades, including most notably deforestation, increased cultivation of rice and other crops, and increased irrigation. Further change is ongoing under population and economic pressures. A major focus of this study is the question of what role different classes of vegetation cover may have in the annual hydrologic yield of the basin and seasonal flows, including the severity of water shortage in the dry season and the severity of floods in the monsoon season. We imposed the additional constraint of requiring the best available estimates of the extent of paddy rice and of irrigated rice.

Data on vegetation cover are needed that are accurate and that cover different historical periods, to represent the evolution of land use over as long a period as possible. An extended survey of the available data sets found six land cover data sets, MODIS-IGBP, AVHRR-UMD, Landsat MSS and TM-TRFIC, AVHRR-OGE, AVHRR-GLC, and AVHRR GLC-SEA (Fig. 2.58). Some data sets are based on the readings of the AVHRR satellite in 1992/93, one is based on readings of the MODIS satellite in 2000/01, and three are based on readings of the Landsat MSS and TM satellites in 1973, 1985, and 1992. Every one of these data sets has a resolution of 1/120-degrees of longitude and latitude, that is, it provides data for every land “pixel” in the Mekong (whole or part) measuring about 1 km x 1 km. Each data set uses a different land cover classification system, that is, the list of land use classes considered (here called the “legend”) is different in each case.

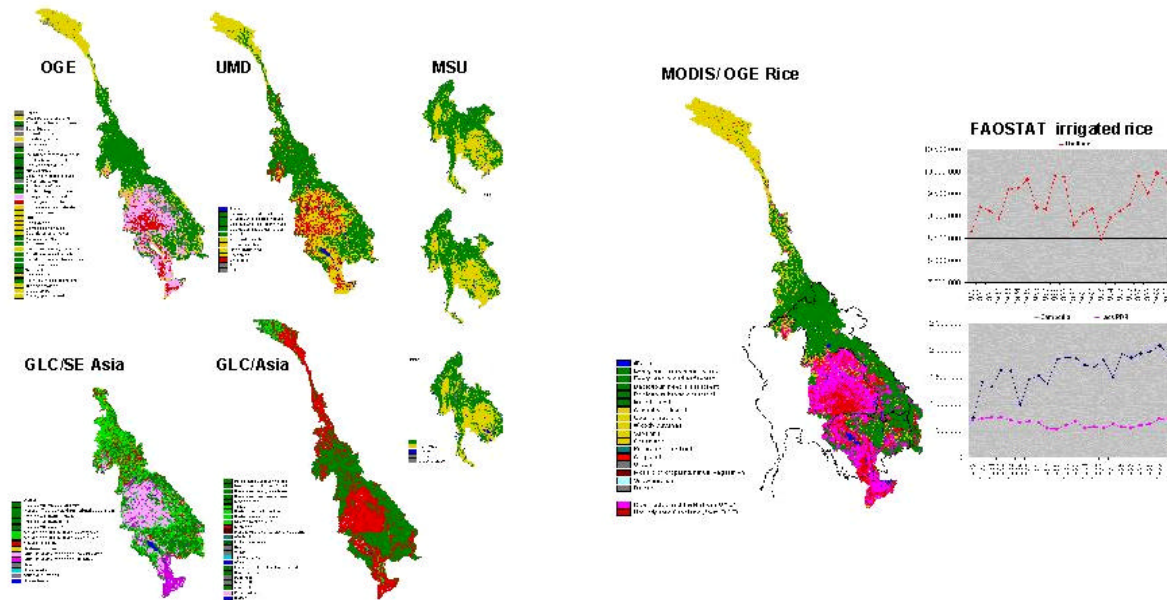


Figure 2.58. (left panel) Different landcover/landuse schemes. (right panel) MODIS Landcover data set used here, combined with OGE Rice and Irrigated Cropland for Landcover Change Hindcasting, with FAOSTAT statistics

With the hope that combination of these data sets would inform us on land cover changes in the period 1973 through 2000/01, we investigated the comparability of the different land cover classification systems. For example, despite land use changes between 1992/93 and 2000/01, if the AVHRR-based data were comparable to the MODIS-based data set, we would expect to find a clear correspondence between classes. For example, pixels classified as covered by “evergreen broadleaf forest” in the University of Maryland (UMD) classification of the AVHRR 1992/93 data, would be expected to maintain, in large number, the same classification “evergreen broadleaf forest” in the IGBP classification of the MODIS 2000/01 data. As we discovered, this turns out not to be the case. We conducted a detailed comparison between the various satellite data sets, and a comparison between the data sets and statistics from FAOSTAT (the World Food and Agriculture Organization data, for the extent of irrigated rice) (Cabral et al in prep).

Faced with general non-comparability between any pair of data sets, despite their different legends, we faced the following questions: a) Which data set most accurately describes land cover at its time of measurement, as compared to FAOSTAT data? b) Which data set uses a land use classification legend that is most informative for the VIC hydrologic model? And, c) once a data set is chosen based on criteria (a) and (b), what is the most reliable method of “re-constructing” a time series of land use classes for our period of study, 1979-2000, and how can we incorporate the FAOSTAT data for that purpose?

In view that, to our knowledge, none of these satellite-based data sets has been validated for Southeast Asia, and given their lack of agreement with FAOSTAT data and with one another, the reasonable approach in our view is to use the satellite-based data sets to aid in identifying spatial distribution of each land use class, but to modify them so as to agree with FAOSTAT values (from Table 2.5).

We choose the MODIS-IGBP data set because: a) Based on the MODIS-satellite readings a data set of leaf area index (LAI) is also available, which can provide us with the monthly LAI values needed for running the VIC hydrologic model (see below). Being able to use vegetation cover and LAI data from the same source provides internal consistency in the data. This consistency is what allows us then to generate reconstructed maps of LAI from the reconstructed maps of land cover. b) The IGBP classification is convenient for us because most of the classes in its legend are the same as in the UMD legend. This is an advantage to us because earlier work at the University of Washington has resulted in the compilation of a library of the vegetation parameters required by VIC, for each of the UMD class.

Because the IGBP classification does not include either rice paddies or irrigated areas, the MODIS-IGBP data set is used in conjunction with AVHRR-OGE class 36, “rice paddies and fields”. Because OGE class 36 over-estimates the extent of rice areas, by a factor estimated to be 2.75 from comparison with FAOSTAT data, we assume that those pixels in this OGE class are those which contain some rice cultivation, but are not necessarily entirely covered by rice. Rather than eliminating almost one in every three rice pixels in order to reach agreement with FAOSTAT, we opted by assigning a fraction of $1 / 2.75$, or 36%, of each OGE class 36 pixel to rice, while the remaining 64% is “cropland” with unspecified crops. The same approach is followed for irrigated rice. FAOSTAT data are used to specify which fraction of rice is irrigated rice; this fraction varies by country. Scenarios were then constructed by changing all croplands to forest, and all forests to croplands.

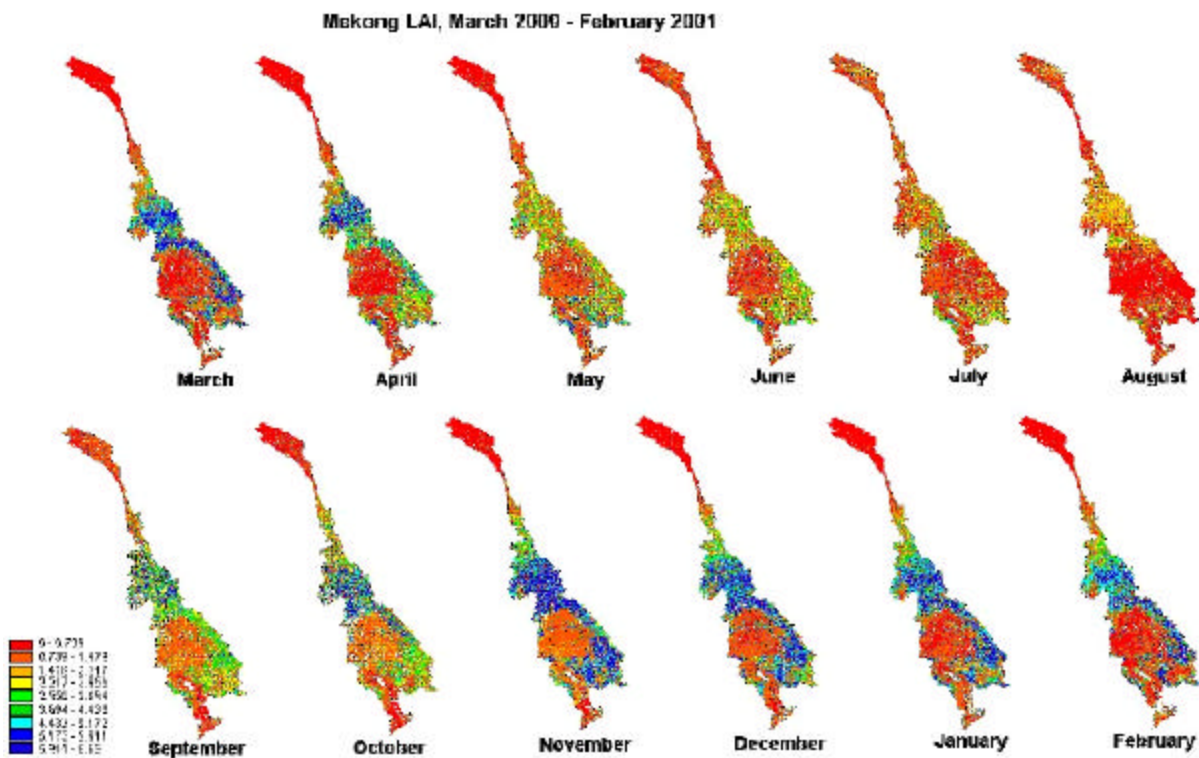


Figure 2.59. Map images of the dataset of 12 monthly mean LAI values obtained from MODIS 2000/01

With this scheme in place, the hydrologic parameters required were assigned. The fraction of roots was assigned in such a way that trees and plants would predominantly take moisture from the top two soil layers. The rooting depths were so specified that only a nominal fraction of the roots extended beyond a depth of 1.0 m. The specification of other vegetation parameters such as height, minimum stomatal resistance, architectural resistance, roughness length, and displacement height was based on Nijssen et al. (2001a).

d) Leaf Area Index (LAI). LAI is required directly by the model. The values of Leaf Area Index (LAI) are those derived from the MODIS satellite readings from 03/01/2000 through 02/28/2001, which have a 1-km resolution, and a time resolution of 8 days. According to the MODIS web page, these LAI data have been evaluated, and are of quality appropriate for use in scientific publications. These data were projected to a geographical grid of 1/120 degrees (which is also about 1 km), and were then aggregated to the model grid of resolution 1/12 by averaging over the area of each model grid cell. Data were also aggregated in time by averaging the two or three 8-day readings for each month. Thus, a dataset of 12 monthly mean LAI values was generated for each model grid pixel, which is displayed in Fig.2.59.

In the hindcast of land cover types back to 1979, rice cultivation was replaced by forest, or vice-versa, according to the census data. When forest (or rice cropland) was inserted, the LAI values were accordingly replaced by those derived from MODIS for the closest pixels having that land cover type in 2000/01. The dominant forest cover type, by far, is “broad leaf evergreen”. Over the entire Mekong basin, the LAI values for this type of forest vary greatly for any given month. For example, Figure 10 shows the mean, minimum and maximum monthly values derived from MODIS 2000/01 for the Mun River sub-basin.

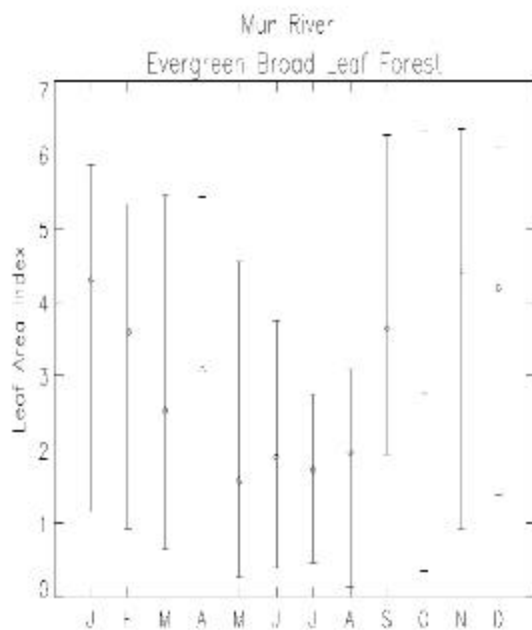


Figure 2.60. Range, and mean of LAI values derived from MODIS 2000/01 averaged over each month, for the Mun River sub-basin.

2.2.7.3. Climate Forcing and Hydrology Data

We have 2 intersecting requirements for climatological data: driving the VIC modeling, and for specific rainfall/discharge analyses (particularly related to floods)

a) Surface Climatology. The meteorological data used to drive the VIC model includes daily values of precipitation, maximum and minimum temperatures, and wind velocity. Station observations of daily precipitation and temperature were obtained from the NOAA Climate Prediction Center Summary of the Day data archived at the National Center for Atmospheric Research for the period January 1979 through December 2000. Data from 279 stations (Fig. 2.61) were interpolated to the model grid cells using the SYMAP algorithm (Shepard, 1984) to obtain daily time series of precipitation and maximum and minimum temperature for each grid cell. Temperature data were interpolated using a lapse rate of $-6.50\text{C}/\text{km}$ to adjust temperature from the station to the grid cell elevations. Wind speed data at $\frac{1}{4}$ degree were obtained by interpolating 2.50×2.50 daily data from NCEP-NCAR Reanalysis (Kalnay et al., 1996) to the $\frac{1}{4}$ degree model grid cells.

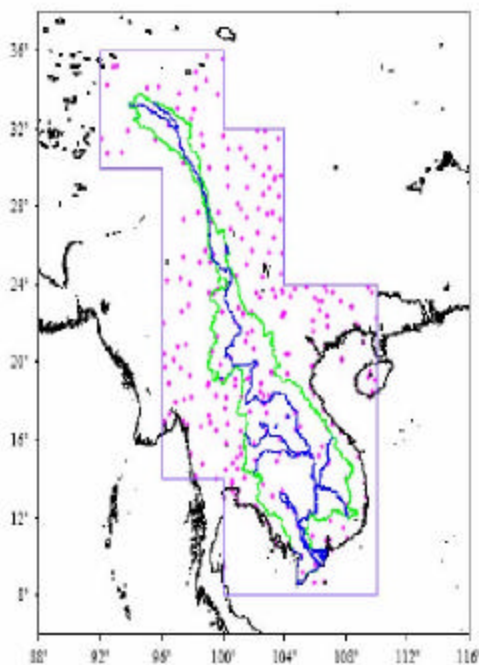


Figure 2.61. Meteorological data stations used for interpolation to surface climatology

For minimum and maximum temperature and wind values, we downloaded the Surface Summary of Day Data (SoD) records from the National Climate Data Center (NCDC). This data is station (point) data and archived in ASCII format. It was determined that 1254 stations are located within a rectangle with lower left corner at 86 degrees East and 12 degrees South and upper right corner at 140 degrees East and 36 degrees North. For the time period January 1997 through September 2000 1368 daily files were constructed for temperature and wind. There were five missing days where by grids were created by temporal interpolation. Although this data also includes precipitation values, it was judged that the gridded data from GPCP and TRMM are superior rainfall products, and thus the SoD precipitation data were not used. The daily point data files for wind and

2.2.8. DHSVM (The Mae Chaem)

Deforestation and upland cultivation in the Mae Chaem watershed in Chiang Mai, Thailand, are believed to be the cause of lowland flooding and lack of dry season water supply. One purpose of this study was to simulate and analyze the historic and current seasonal and annual characteristics of hydrologic response in Mae Chaem. The second objective was to forecast the stream flow regime and annual water yield based on three future scenarios of land-use change, with the focus on the conversion from forest to croplands and *vice versa*. Because the agriculture in this region relies on irrigation, the comparisons of the results both with and without irrigation diversion were considered. The project also aims to evaluate the far-field effect of stream flow due to the spatial variation in land-use change. This modeling work can be a useful tool for water resource management and flood forecasting for small catchments undergoing rapid commercialization.

2.2.8.1. DHSVM: The Hydrology Model.

The physics as represented by the Variable Infiltration Capacity (VIC) model (Section 2.2.7) would not accurately represent the steep topography and finer-scale issues of the Mae Chaem basin. As noted, VIC is conceptualized as a larger, regional scale model. As such, its application to smaller-scale basins and sub-basins, such as the Mae Chaem, is questionable. So to examine problems at this scale, we opted to use a higher resolution hydrologic model, the Distributed Hydrology Soil Vegetation Model (DHSVM, Wigmosta *et al*, 1994) (Fig. 2.63). Unlike VIC, DHSVM is intended for small to moderate drainage areas (typically less than about 1000 km²), over which digital topographic data allows explicit representation of surface and subsurface flow. Like VIC, it represents runoff generation via the saturation excess mechanism. Unlike VIC, it explicitly represents topographic effects, including the formation of perched water tables on runoff generation and incident solar radiation (hence net radiation), as well as vegetation and its properties (like root depth) and soil parameters, on a pixel-by-pixel basis. The model grid resolution typically is 30-150 m, several orders of magnitude higher than VIC. However, because of the large computational burden (and data limitations), DHSVM is restricted to relatively small catchments. We have conducted some limited experiments comparing the sensitivity of DHSVM and VIC to vegetation change (Van Shaar *et al*, 2002). Although the macroscale performance of the two models is similar in gross features (e.g., ability to reproduce seasonal fluctuations in runoff), there are important differences in predicted runoff and other surface fluxes, especially at shorter time scales.

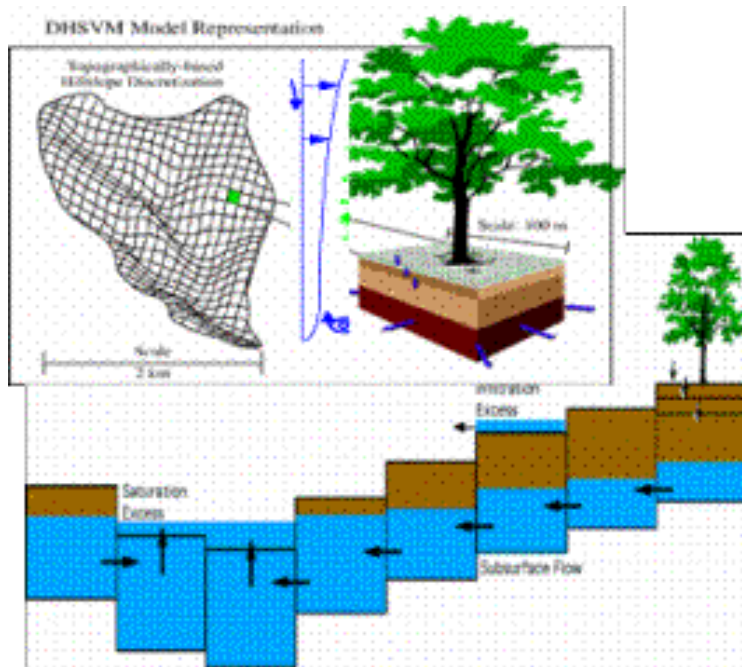


Figure 2.63. A schematic of the DHSVM (Distributed Hydrology Soil Vegetation Model)

2.2.8.2 Development of the Geospatial Model of the Mae Chaem Basin

Sharp vegetation and relief (and relatively sparse data) characterize the Mae Chaem (Chaem River) watershed. The total basin area above river gage station P.14, operated by the Royal Irrigation Department (RID) is 3,853 km². The basin has a wide range of elevation, with the highest peak at Doi Inthanon (Mount Inthanon) summit, 2535 m.a.s.l. and the lowest point is 282 m.a.s.l. (Kuraji *et al.*, 2001). The altitude variation induces different climatic zones and distinctive types of natural land cover. The dominant vegetation are dry dipterocarp and mixed deciduous forests below 1000 m, tropical pine forest from 900 – 1500 m, hill evergreen forest at higher elevations up to 2000 m, and Tropical montane cloud forest above 2000 m (Dairaku *et al.*, 2000 and Kuraji *et al.*, 2001). The sloping hillsides are one common landscape element, with maximum slope inclination more than 25%. This feature leads to natural soil erosion and prevents advanced soil development. Therefore, the soil horizon is relatively shallow and has limited water-holding capacity (Soil survey and Hansen, 2001).

Flow Network . The topography for the Mae Chaem was initially obtained as a 30-m digital elevation model (DEM), acquired from the International Center for Research in Agroforestry (ICRAF), Chiang Mai. This 30-m DEM was then aggregated to 150-m resolution (Fig. 2.64) using a mean calculation. The flow direction, flow accumulation, and stream network were derived from the DEM at 150-m resolution. The soil depth was generated by DHSVM, based on the DEM and was adjusted during model calibration.

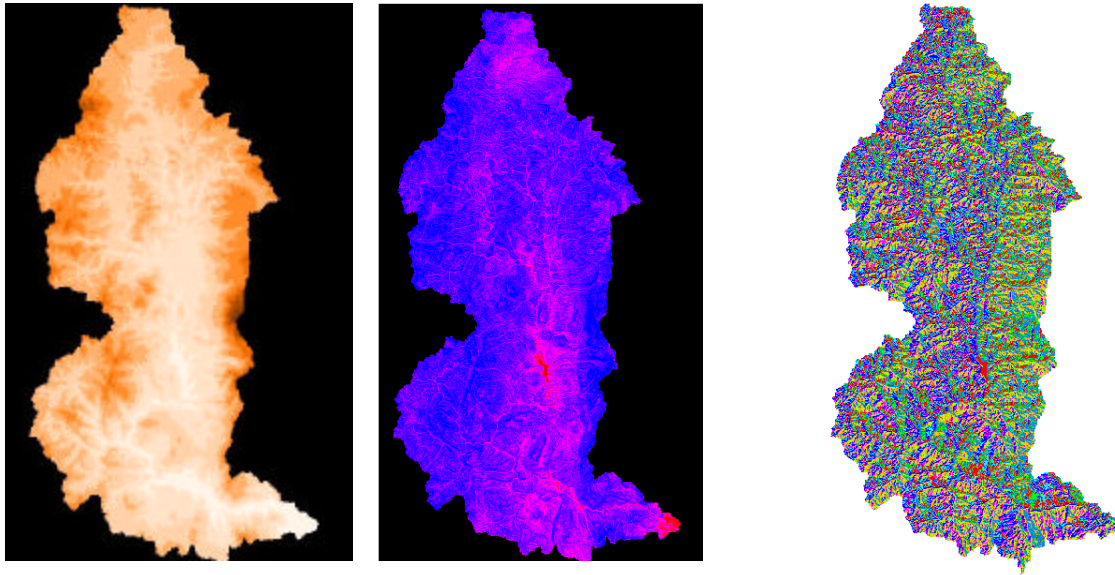


Figure 2.64. Mae Chaem topography, soil depth, and flow direction grids (left to right) represented by the 150-m DEM

Soil map and attributes. Soil data in the Mae Chaem are very sparse and restricted to the lowlands. Therefore, a soils map containing physical and chemical properties was extracted from the Soildata program. This program generates 5-minute resolution soil data based on the Global Soil Database developed by the ISRIC and FAO. The soil map was resampled to 150-m resolution.

Vegetation and Land Use. Two landcover datasets form the basis for the landcover change scenarios in the hydrology model. The original classification schemes of these data vary significantly, so modifications were made to the schemes to achieve similarity between the landcover data. The first dataset in the time series is a historical 1989 dataset (Fig. 2.65a), acquired from the Land Development Division (LDD), Ministry of Agriculture, Thailand. This data, originating as polygons, was converted to a 150m raster grid representation using a nearest-neighbor assignment algorithm. The data was then generalized into 11 classes (Fig. 2.65c), from its original 47. The second dataset represents landcover for the year 2000, referred to as the current landcover (Fig. 2.65b). This dataset, also from the LDD, was prepared for our model using the same procedure as that of the 1989 data. However, the original 47 class names in this dataset differed from those in the 1989 data. We reconciled the class names by performing a combinatorial analysis between the 1989 reclassified dataset and the 2000 original data. In this way we were able to establish a correlation between the 11 classes in 1989 and the 47 original classes in 2000. This type of spatial overlay analysis returns not only the frequency of all unique combinations of landcover type, but also a map product of the spatial commonalities. A plot was made to identify the frequency of occurrence between a 2000 value (1 to 47) and a 1989 value (1 to 11). Based on this plot, the 2000 vegetation values were re-assigned a value consistent with the frequency distribution of shared space with the 1989 dataset (Fig. 2.65d).

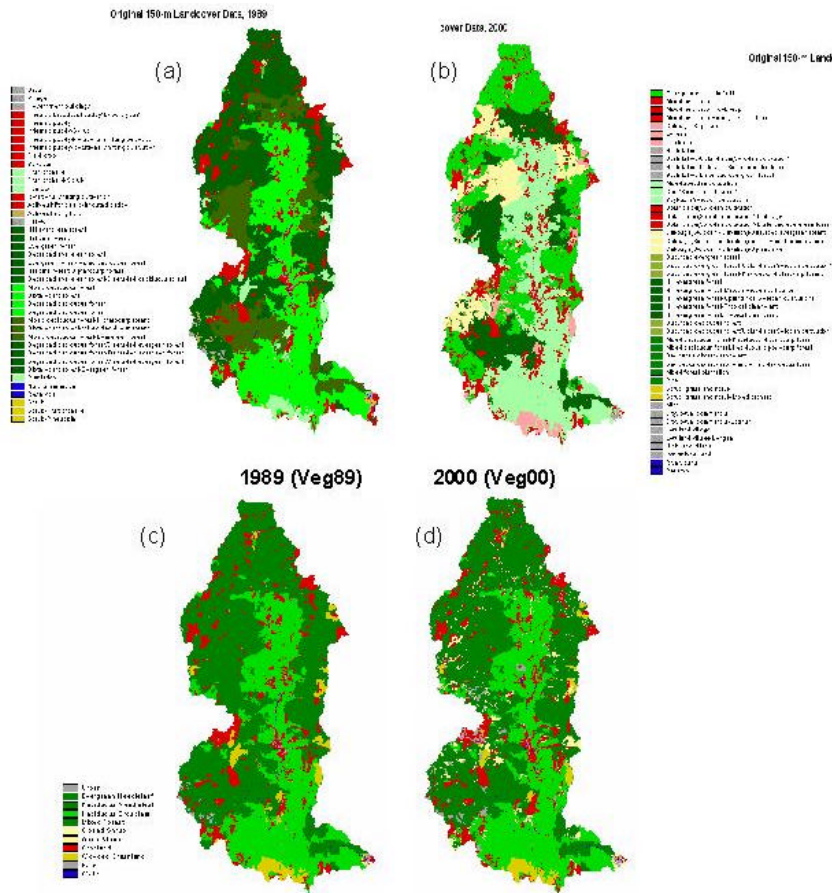


Figure 2.65. Mae Chaem landcover (a) original 1989 historical, (b) original current 2000, (c) re-processed 1989, (d) re-processed 2000 data sets

Future Scenarios. Five future scenarios, forecasted to the year 2010, were created with a focus on the conversion of cropland to forest (Fig. 2.66). The first scenario represents the reversal of all cropland back to evergreen needleleaf forest in the area above 1000 m.a.s.l., and to deciduous broadleaf forest below 1000 m.a.s.l. The second scenario depicts the replacement of all forest types (class 2-5) to croplands above a strategic point A. This point was chosen because of its location on the main stem above which the largest portion of forests changed to croplands from 1989 to 2000 (see section 4.3.3 for details). The third scenario forecasts the doubling of cropland area from 2000 by growing a buffer of new crop cells around all existing crop patches. This ultimately increased the total basin area of cropland from 10.4% in 2000 to 19.9% in 2010 (Table 2.6). Finally, the fourth and fifth scenarios depict a doubling of cropland that is limited to either the highland basin (above 1000 m.a.s.l), or to the lowland basin (below 1000 m.a.s.l). Growth of cropland limited to the highland basin increased the total basin area of crops to 18.0%, while growth of lowland crops increased the total basin area of cropland to 19.1% (Table 2.6). In both cases, a buffer was grown around existing crop patches in the selected elevation range, while crop patches in the unselected elevation range remained the same as in 2000.

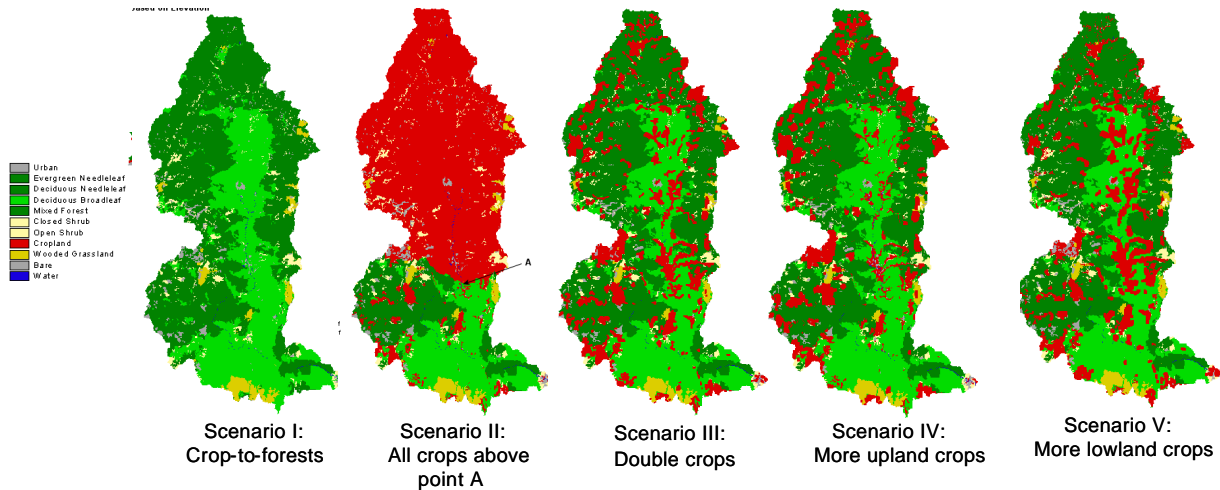


Figure 2.66. Landuse conversion scenarios

Table 2.6. Summary of total crop areas in all land cover data sets.

Land cover set	% Croplands in the basin
1989	10.3
2000	10.4
Scenario I: Crop-to-forest	0
Scenario II: All crops above point A	62
Scenario III: Double crops	19.9
Scenario IV: More upland crops	18.0
Scenario V: More lowland crops	19.1

2.2.8.3. Climate Forcing and Hydrology Data

a) Climatology. Daily rainfall and maximum and minimum air temperature records for the period of 1993-2000 were available from five meteorological stations and one agrometeorological station (Table 1). Doi Inthanon (DO) and Wat Chan (WA) stations are operated by the Royal Project Foundation, and the secondary data was obtained from both ICRAF and the Royal Project Foundation. The Research Station (RE) belongs to the Gewex Asian Monsoon Experiment-Tropics (GAME-T), led by the University of Tokyo, Japan. Mae Jo Agromet (TMD327301), Mae Hong Son (TMD300201) and Mae Sariang (TMD 300202) stations are managed by the Thai Meteorological Department (TMD). Sub-daily interpolation of temperature, radiation, and humidity were generated by compiling the VIC model to only output sub-daily climate data (Maurer *et al.*, 2002). The wind speed is assumed to be 2 m/s for all stations, except for RE and TMD327301, which have average daily wind speed records. The vegetation and soil parameters used for computing the disaggregated climate records were taken from VIC sample data (http://www.hydro.washington.edu/Lettenmaier/gridded_data/forcing_data_sample.html).

This algorithm assumes that the total daily rainfall is evenly distributed through the sub-daily intervals. We then replaced the calculated 3-hour precipitation in 1998 – 2000 by observed records for all TMD stations.

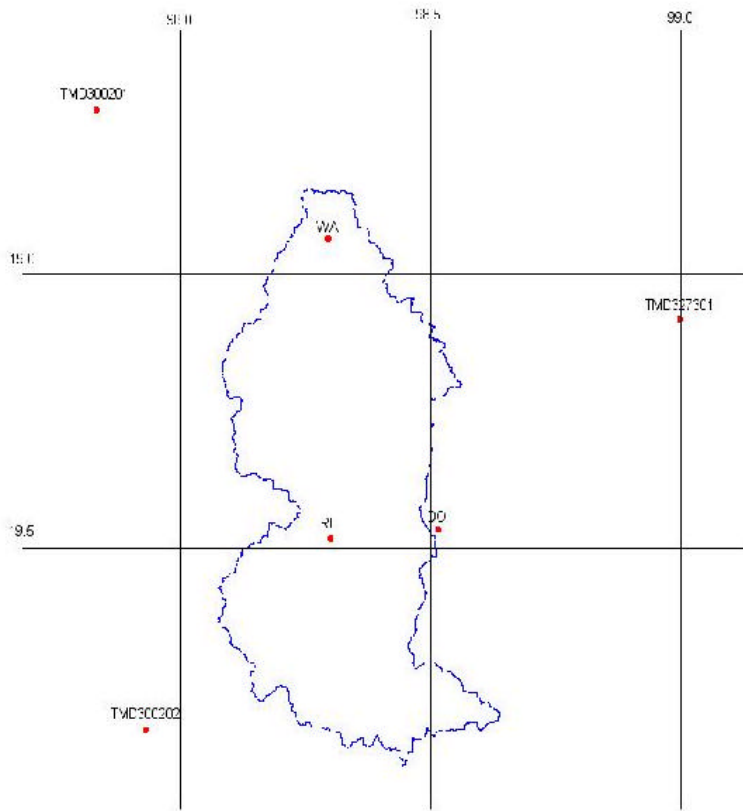


Figure 2.67. Map of climate stations

Table 2.7. Location and elevation of climate forcing stations

Station name	Altitude(m.a.s.l.)	Latitude (N)	Longitude (E)
Wat Chan (WA)	990	19 ° 04'	98 ° 17'
Doi Inthanon (DO)	2565	18 ° 35'	98 ° 29'
Research Station (RE)	1100	18 ° 31'	98 ° 18'
Mae Hong Son (TMD300201)	267	19 ° 18'	97 ° 50'
Mae Sariang (TMD 200202)	212	18 ° 10'	97 ° 56'
Mae Jo Agromet (TMD327301)	490*	18 ° 55'	99 ° 00'

* Estimated from DEM.

b) Stream flow. Daily average stream flow measurements were acquired for the basin outlet at Kaeng Ob Luang (gage P.14), operated by the Royal Irrigation Department.

2.3 Plausible land use change scenarios for northern Thailand

To make the land use change scenarios that are to be evaluated more realistic, a link was made to ongoing studies for the Millennium Ecosystem Assessment for the Mekong basin. These scenarios both help guide the generation of future landscapes as well as provide context in which to interpret the implications of modeled outcomes. The main value comes in their comparison rather than the plausibility of individual scenarios.

A set of four scenarios was developed for the Upper Ping River Basin placing emphasis on contrasting evolution of amount and spatial distribution of land cover (Fig. 2.68). The four scenarios, “***Fields and Fallow***”, “***Food Bowl***”, “***Parks and Cities***” and “***Agro-forests***”, in turn, can be thought of as being nested in larger scale scenarios about national and regional global development, here given alternative names (larger boxes in which main scenarios are nested). These larger scale scenarios are not discussed in detailed here, but were intentionally constructed to as consistent as possible with those being developed by Global Scenarios working group of the Millennium Ecosystem Assessment. The scenarios at both scales differ in the assumptions they make about economic development and social organization (Fig. 2.69 and 2.70).

In this study the four scenarios for the Ping Basin were applied to the Mae Chaem sub-basin. This was done in three steps.

- First, historical analysis of land-use change over the past 10 and 20 years were made using multiple regression techniques. This required substantial effort at acquiring and preparing datasets. In the end we adopted a consistent 1km and 10km grid-based system to facilitate future cross-scale work for variables measured at various resolutions. With the gridded system land-covers take on % cover values for each cell.
- Second, soft models were constructed to make explicit some of the main assumptions underlying each of the scenarios and how they could be articulated in a quantitative landscape evolution model (Fig. 2.70).
- Third, a platform for modelling and visualization landscape evolution was built in Visual C++. This allowed us to both include systems of differential equations based on regressions of land-use change on a set of categorically transformed predictor variables and rule-based processes. The first version of the model with which the set of simulated landscapes presented here is based largely on modifying small subsets of the underlying regression coefficients guided by the soft models. Land-covers modelled were: orchard, paddy, field crop, hi-value intensified crop, fallow/secondary shrub, human settlements. Other land-uses such as water bodies were assumed to stay constant. Predictor variables were similar to those shown in the soft model diagrams (Fig. 2.71), including, for example, elevation, past land use, estimates of travel times and distance to water.

Table 2.8. Steps in the scenario development for Mae Chaem as part of the Ping river basin

<p>Main steps in Preparation of the Scenarios narratives and landscape maps.</p> <ul style="list-style-type: none">➤ Analysis of Historical Transitions to Derive Key Relationships➤ Analysis of highly aggregated trends between land-use and other development statistics for the Ping River Basin (Chiang Mai Province/Lamphun as focus)➤ Spatial analysis of historical transitions for much more limited set of variables – using disaggregation algorithms and multi-scale regressions (eg. As in CLUE framework);➤ Detailed analysis of LU changes in Mae Chaem to develop rules for different kinds of upland areas➤ Preparation of set of key constraint layers (elevation, river-network, main cities, infrastructure) to use evolving the landscape <p>Scenario Set</p> <ul style="list-style-type: none">➤ Liaison with users on primary axes to explore “scenario space” based on preliminary set (initial work on proposed framework in Fig. 2.68)➤ Finalize the framing scenarios with storylines➤ Land-use evolution models➤ Develop conversion rules and variants for each scenario (ie. Land-use change models)➤ Evolve landscapes under each scenario with snapshots➤ Derive various landscape metrics at different scales to describe landscape structures -> revisions or variants of scenarios
--